ATLAS measurements of transverse and longitudinal flow fluctuations

Phys. Rev. C 101 (2020), 024906 arXiv:2001.04201

Arabinda Behera

For the ATLAS Collaboration

3rd June, 2020

Hard Probes 2020

Flow - Flow and Decorrelation

- Initial state fluctuations - FB asymmetry in eccentricities

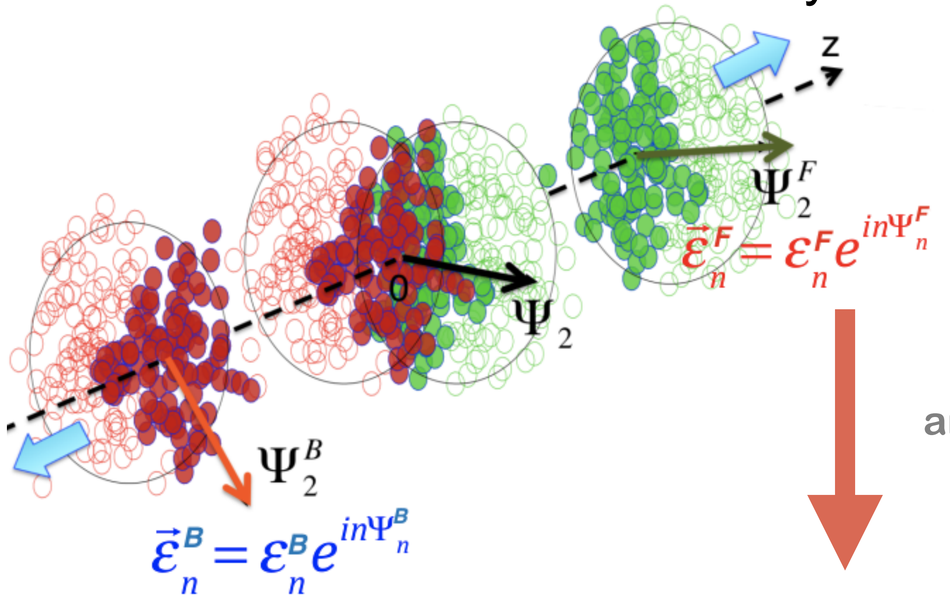

$$\vec{\epsilon}_n^F \neq \vec{\epsilon}_n^B$$

$$\vec{\epsilon}_{n+} = (\vec{\epsilon}_n^F + \vec{\epsilon}_n^B)/2 \Longrightarrow \quad \text{Average Flow}$$

$$\vec{\epsilon}_{n-} = (\vec{\epsilon}_n^F - \vec{\epsilon}_n^B)/2 \Longrightarrow \text{Longitudinal Fluctuation}$$

arXiv:1701.02183

Flow - Flow and Decorrelation

- Initial state fluctuations - FB asymmetry in eccentricities

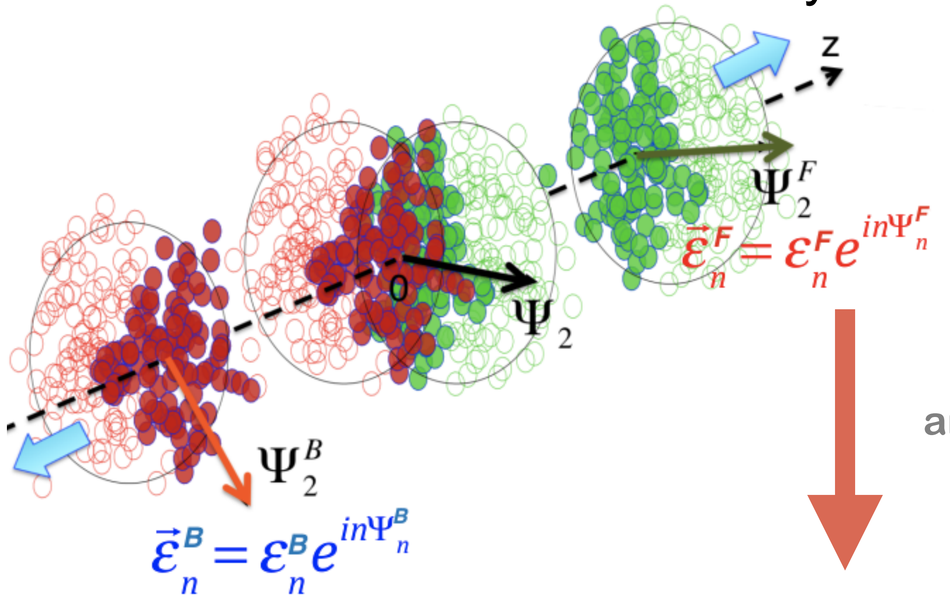

$$\vec{\epsilon}_n^F \neq \vec{\epsilon}_n^B$$

$$\vec{\epsilon}_{n+} = (\vec{\epsilon}_n^F + \vec{\epsilon}_n^B)/2 \Longrightarrow \quad \text{Average Flow}$$

$$\vec{\epsilon}_{n-} = (\vec{\epsilon}_n^F - \vec{\epsilon}_n^B)/2 \Longrightarrow \text{Longitudinal Fluctuation}$$

arXiv:1701.02183

- Hydro evolution of QGP (3+1D)

$$\vec{v}_n = \kappa_n \vec{\epsilon}_n \qquad \vec{v}_n(\eta) = v_n(\eta) e^{in\Psi_n(\eta)}$$

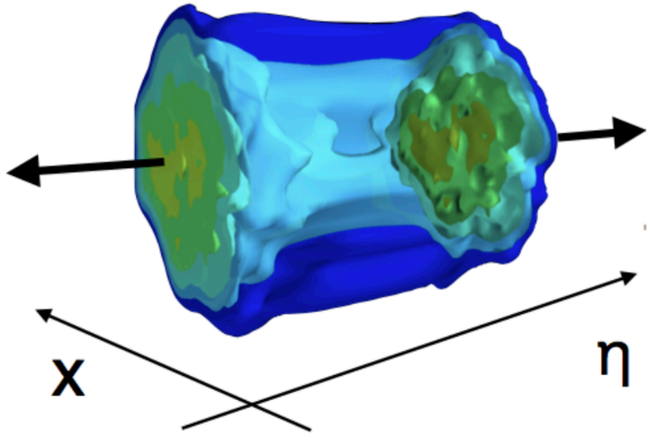

- Final State - average v_n and v_n decorrelation

$$\vec{v}_n(\eta) \approx \vec{v}_n(0)(1 + \alpha_n \eta) e^{i\beta_n \eta}$$

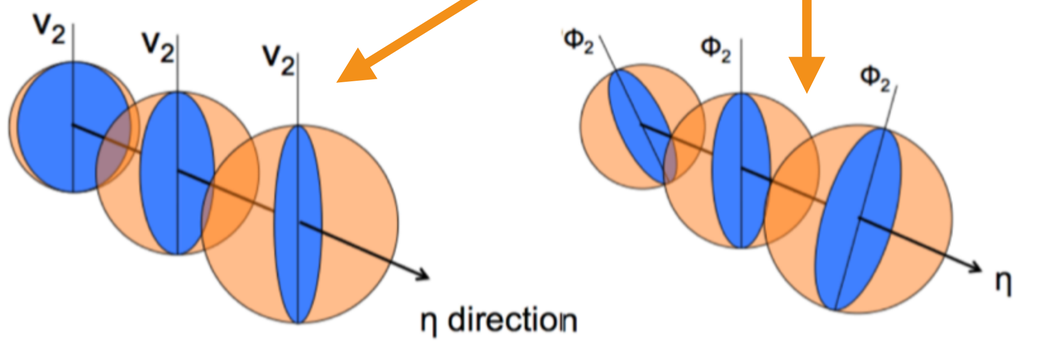

$$v_n(\eta_1) \neq v_n(\eta_2) \qquad \Psi_n(\eta_1) \neq \Psi_n(\eta_2)$$

System-size Dependence

Pb+Pb

A=208, R=6.62 fm

$\sqrt{s_{\mathrm{NN}}} = 5.02\,\mathrm{TeV}$

Xe+Xe

A=129, R=5.42 fm

$\sqrt{s_{\mathrm{NN}}} = 5.44\,\mathrm{TeV}$

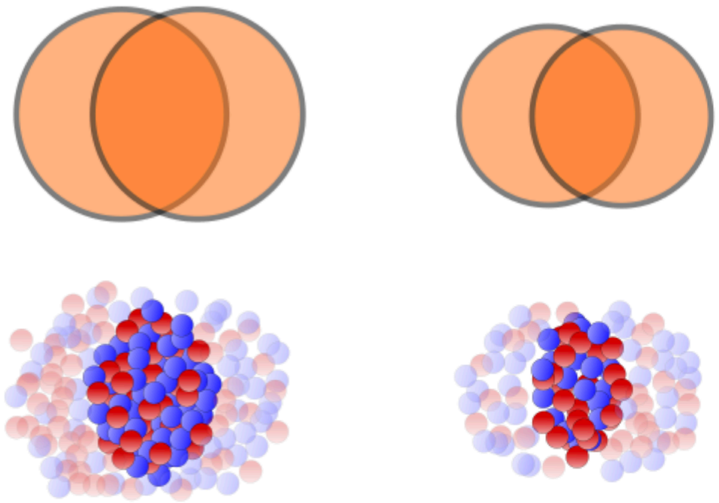

- Different factors can affect the v_n and decorrelation -
  - Initial state geometry
  - Initial momentum anisotropy
  - Shear viscosity
  - Hydrodynamic fluctuations
- How flow and decorrelation are related?
- What is the effect of nuclear deformation (Xe+Xe)?
- Is the dependence same for different harmonics?
- How to disentangle early-time and late-time effects?

✦System-size dependence of v_n and v_n decorrelation : Xe+Xe vs Pb+Pb

✦Ratio between the two systems - disentangle initial and final-state contributions

Centrality dependence - Xe+Xe vs Pb+Pb

- Method - 2-particle correlation technique

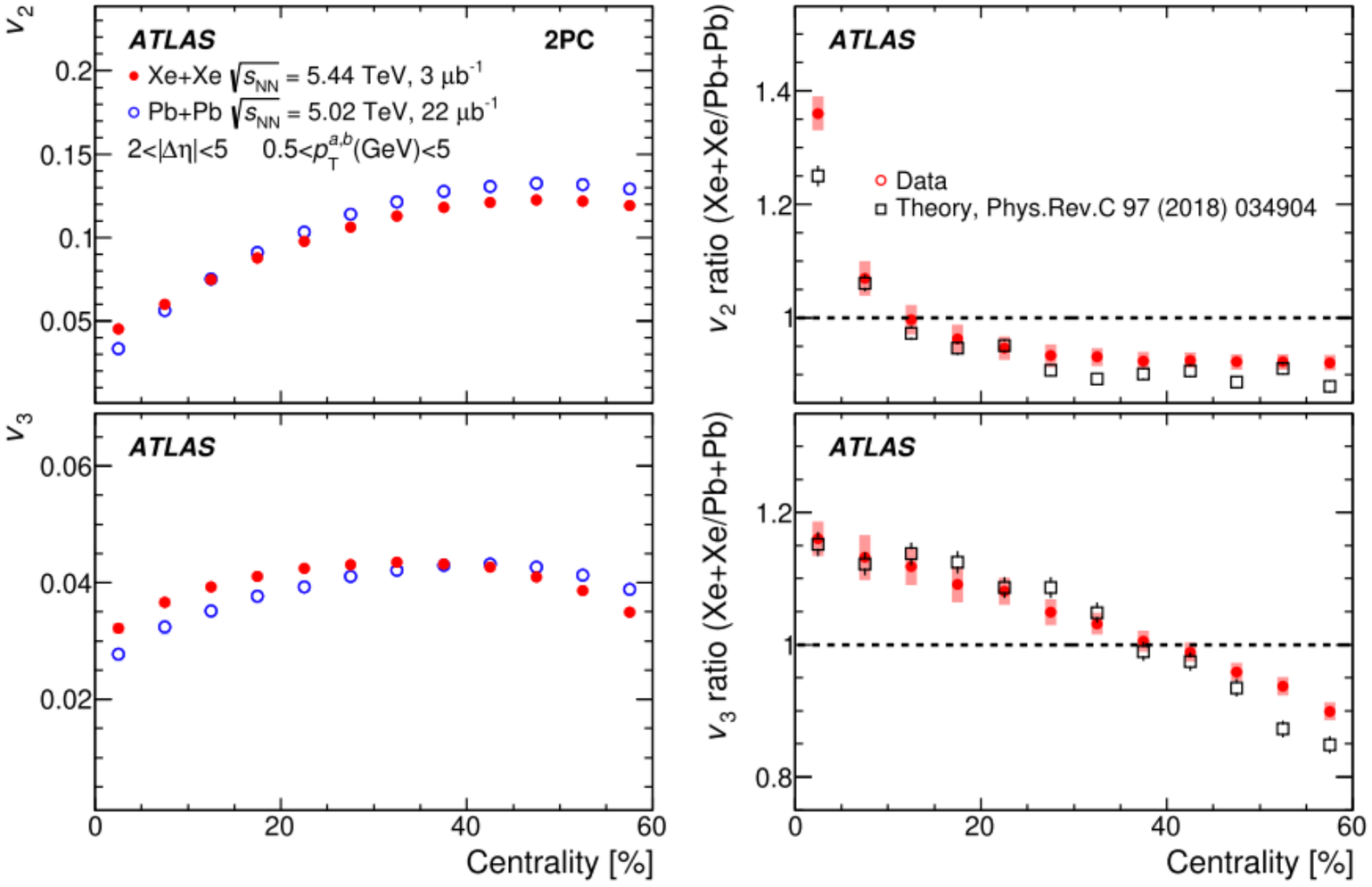

v_2

- Most Central events - Xe+Xe v_2 > Pb+Pb v_2
- From central to mid-central events, the ratio for v_2 decreases, becomes < 1 after 15% centrality
- Peripheral events - ratio seems to saturate

v_3

- Similar qualitative trends
- Ratio < 1 after 35% centrality

- Central - Geometry dominates, Non-central - Viscous effect dominates

N_{part} and N_{ch} dependence - Xe+Xe vs Pb+Pb

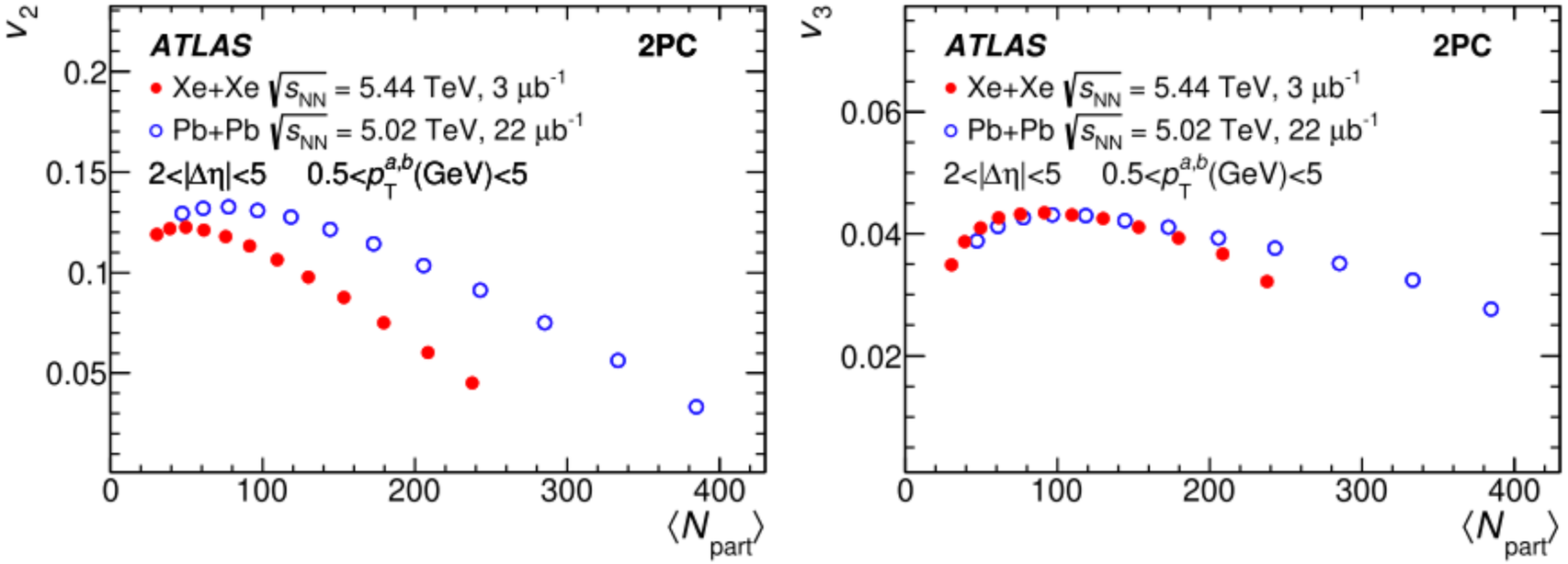

- v_2 - smaller in Xe+Xe than Pb+Pb
- v_3 - similar values except in large N_{part}
- Low N_{part} - all v_n similar values between Xe+Xe and Pb+Pb

N_{part} and N_{ch} dependence - Xe+Xe vs Pb+Pb

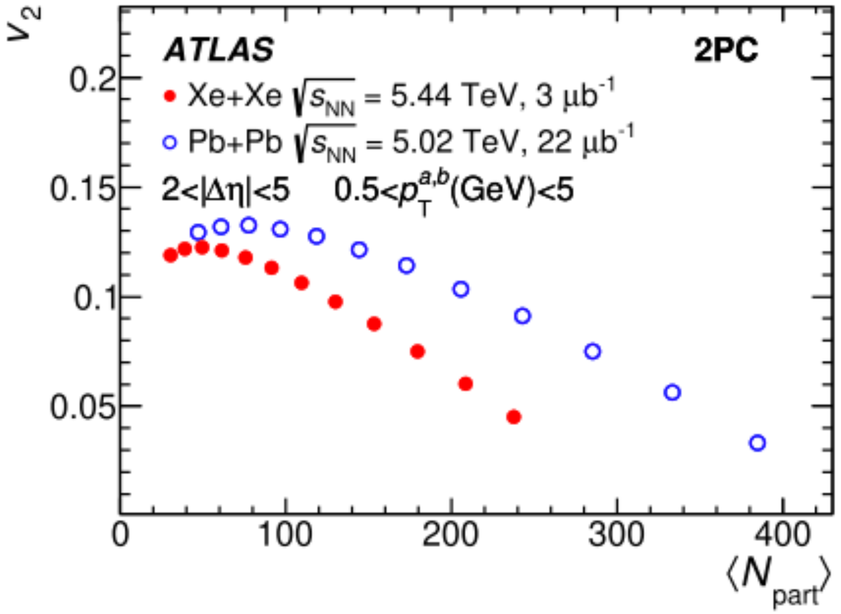

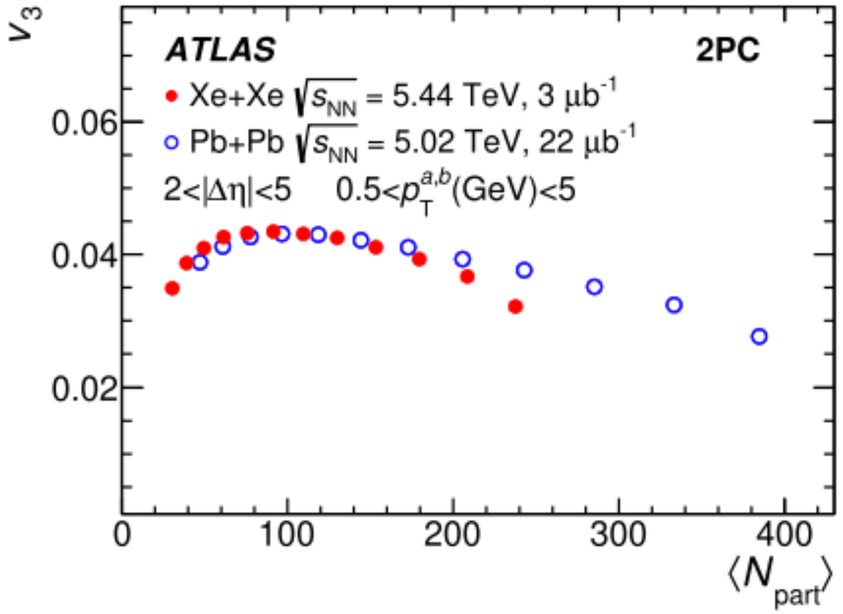

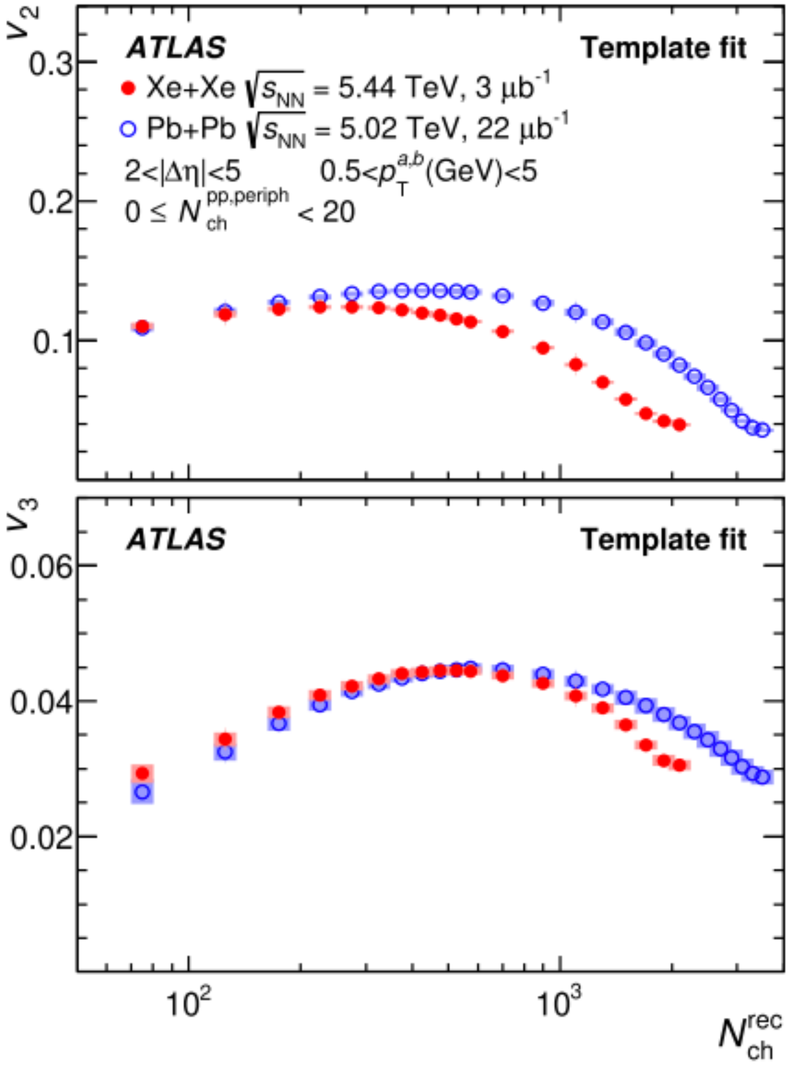

- v_2 - smaller in Xe+Xe than Pb+Pb
- v_3 - similar values except in large N_{part}
- Low N_{part} - all v_n similar values between Xe+Xe and Pb+Pb
- N_{ch} dependence - follow similar behavior as N_{part}

Decorrelation Method

- Flow vector

$$\mathbf{q}_n \equiv \Sigma_j w_j e^{in\phi_j} / (\Sigma_j w_j)$$

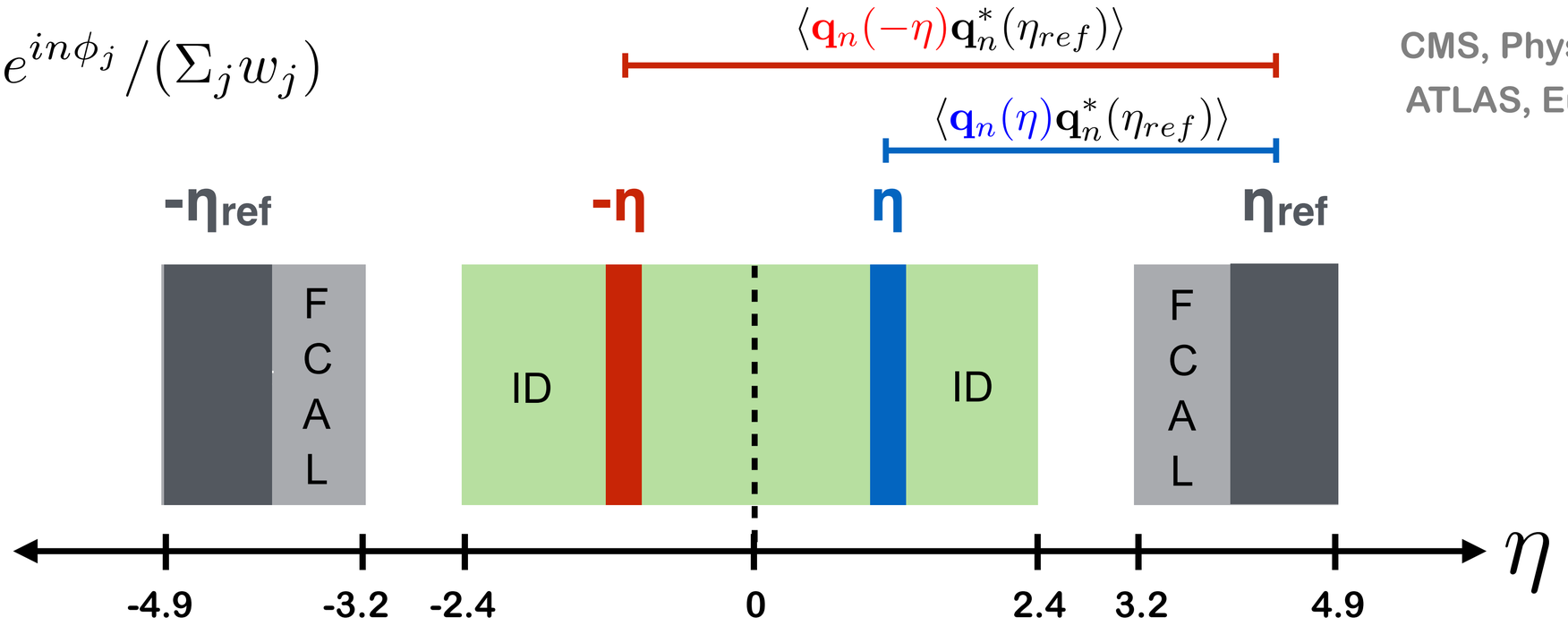

CMS, Phys. Rev. C 92, 034911

ATLAS, Eur. Phys. J. C (2018) 78:142

$$r_{n|n}(\eta) = \frac{\langle \mathbf{q}_n(-\eta)\mathbf{q}_n^*(\eta_{ref})\rangle}{\langle \mathbf{q}_n(\eta)\mathbf{q}_n^*(\eta_{ref})\rangle} = \frac{\langle v_n(-\eta)v_n(\eta_{ref})\cos n(\Psi_n(-\eta) - \Psi_n(\eta_{ref}))\rangle}{\langle v_n(\eta)v_n(\eta_{ref})\cos n(\Psi_n(\eta) - \Psi_n(\eta_{ref}))\rangle} \qquad r_{n|n}(\eta) \leq 1$$

Measures decorrelation between -η and η

Decorrelation in Xe+Xe

- $r_{2|2} > r_{3|3} > r_{4|4}$ - Linear decrease with η
- $r_{2|2}$ strong centrality dependence - larger in mid-central
- $r_{3|3}$ and $r_{4|4}$ - weak centrality dependence
- Similar behavior as 5 TeV Pb+Pb

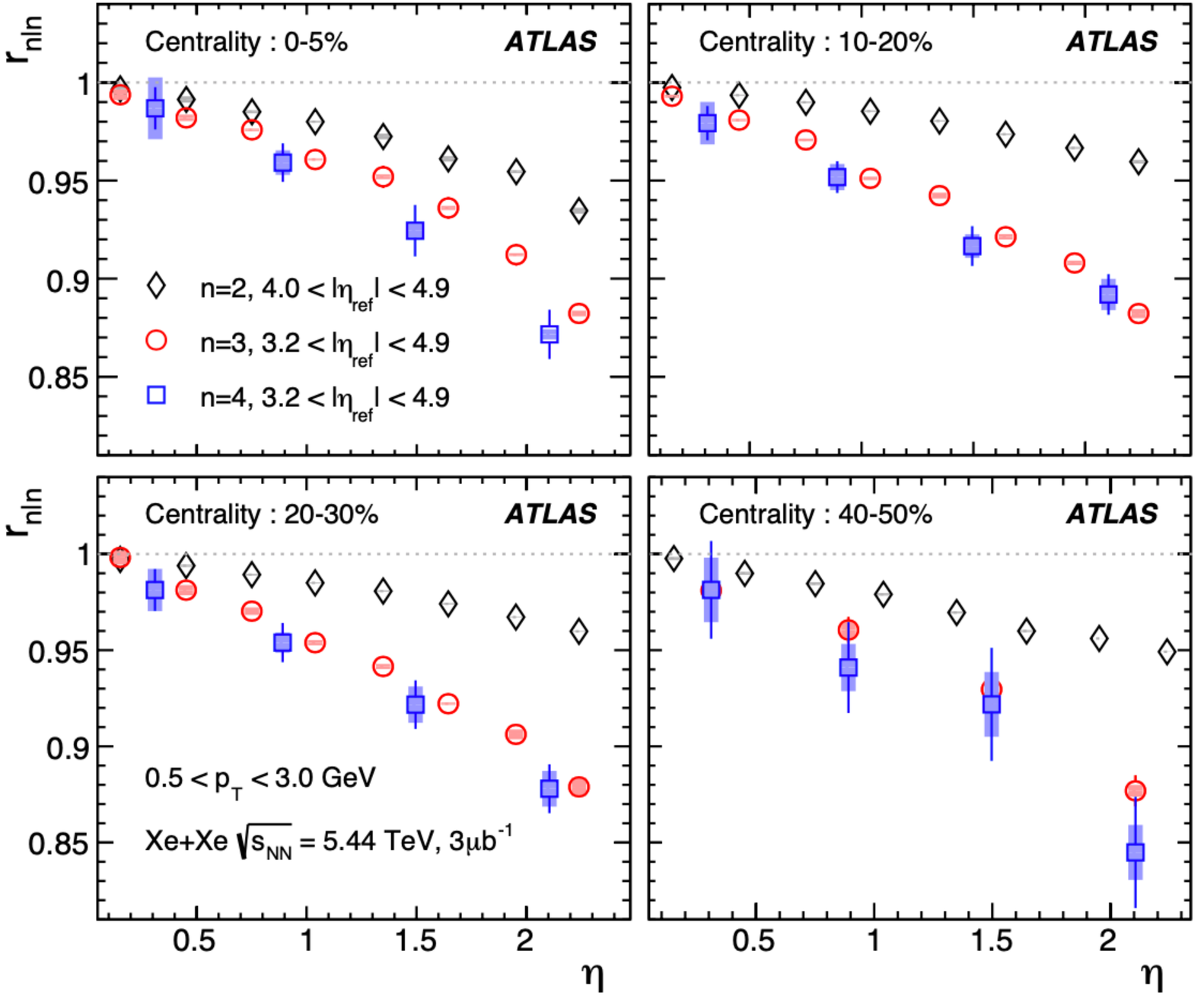

Decorrelation in Xe+Xe

- $r_{2|2} > r_{3|3} > r_{4|4}$ - Linear decrease with η
- $r_{2|2}$ strong centrality dependence - larger in mid-central
- $r_{3|3}$ and $r_{4|4}$ - weak centrality dependence
- Similar behavior as 5 TeV Pb+Pb
- Slope F_n :

$$r_{n|n}(\eta) = 1 - 2F_n\eta$$

Decorrelation strength

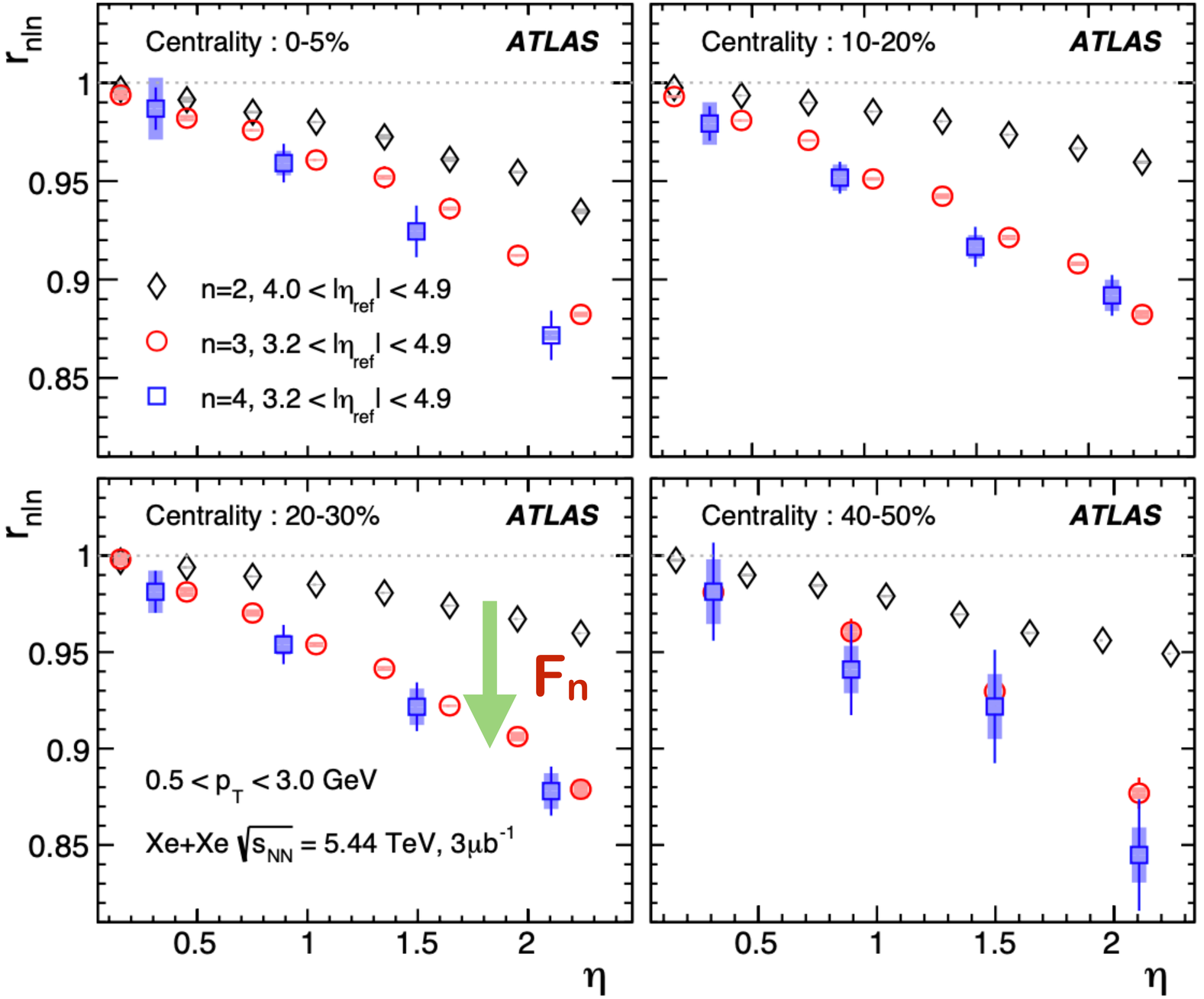

Slope F_n - $|\eta_{ref}|$ and p_T dependence

- Non-flow (dijets) at small $|\eta_{ref}|$ or large p_T

$$r_{n|n}(\eta) = \frac{\langle \mathbf{q}_n(-\eta)\mathbf{q}_n^*(\eta_{ref})\rangle}{\langle \mathbf{q}_n(\eta)\mathbf{q}_n^*(\eta_{ref})\rangle} \uparrow \text{NF} \Rightarrow F_n \uparrow$$

- Larger F_2 at smaller $|\eta_{ref}|$ - NF

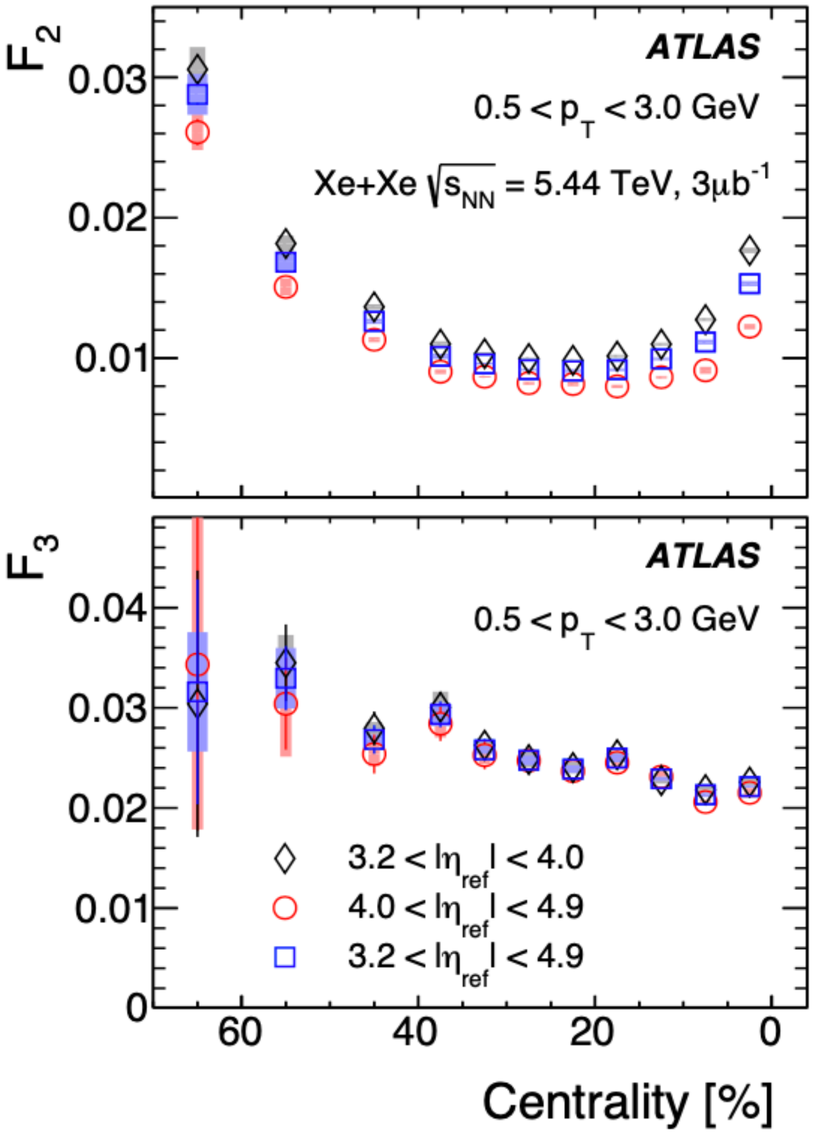

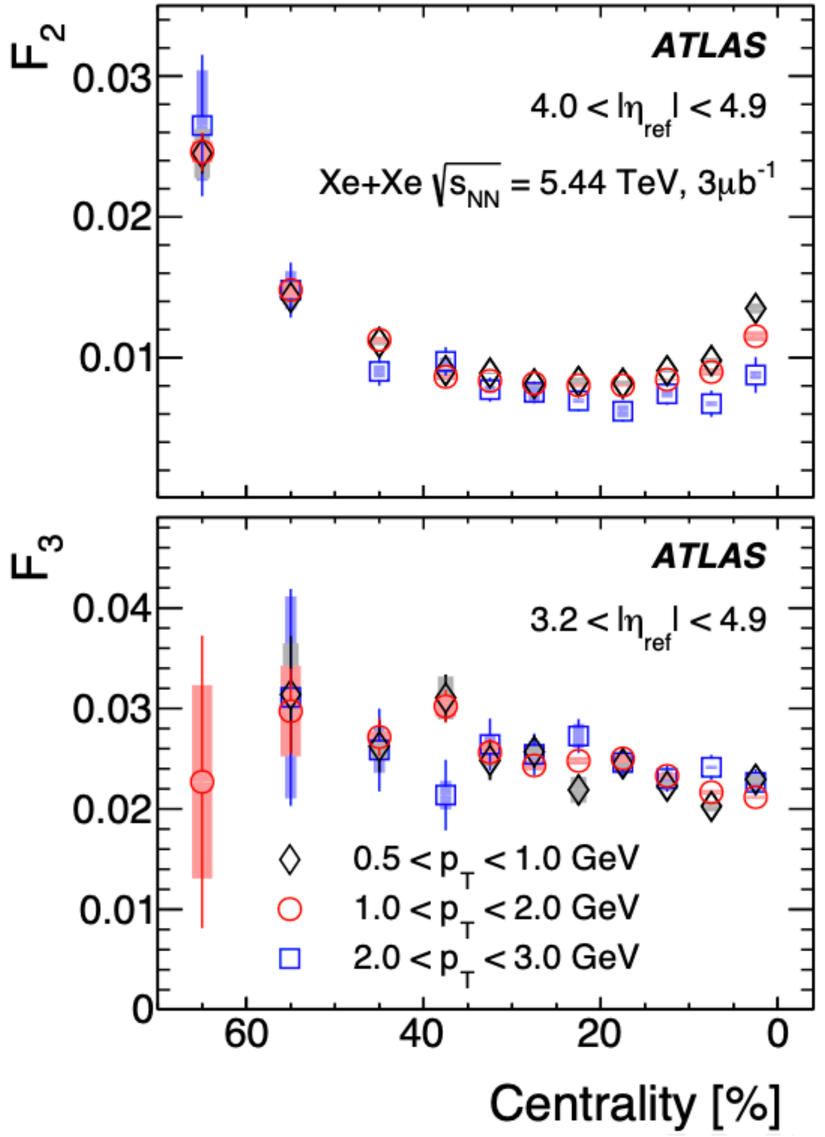

Slope F_n - $|\eta_{ref}|$ and p_T dependence

- Non-flow (dijets) at small $|\eta_{ref}|$ or large p_T

$$r_{n|n}(\eta) = \frac{\langle \mathbf{q}_n(-\eta)\mathbf{q}_n^*(\eta_{ref})\rangle}{\langle \mathbf{q}_n(\eta)\mathbf{q}_n^*(\eta_{ref})\rangle} \uparrow \text{NF} \Rightarrow F_n \uparrow$$

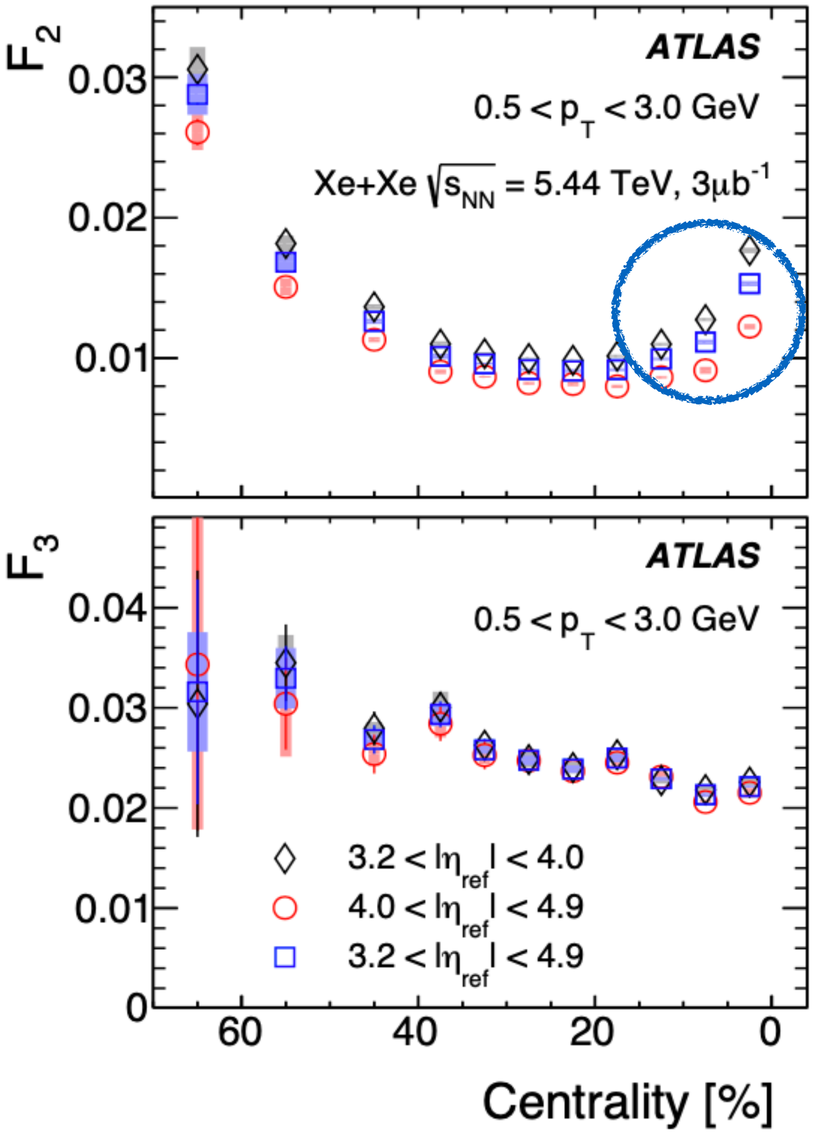

- Larger F_2 at smaller $|\eta_{ref}|$ - NF
- Smaller F_2 at larger p_T - not NF
- Effect larger in central collisions - could be due to non-linear v_2 decorrelation
- F_3 - not affected by NF

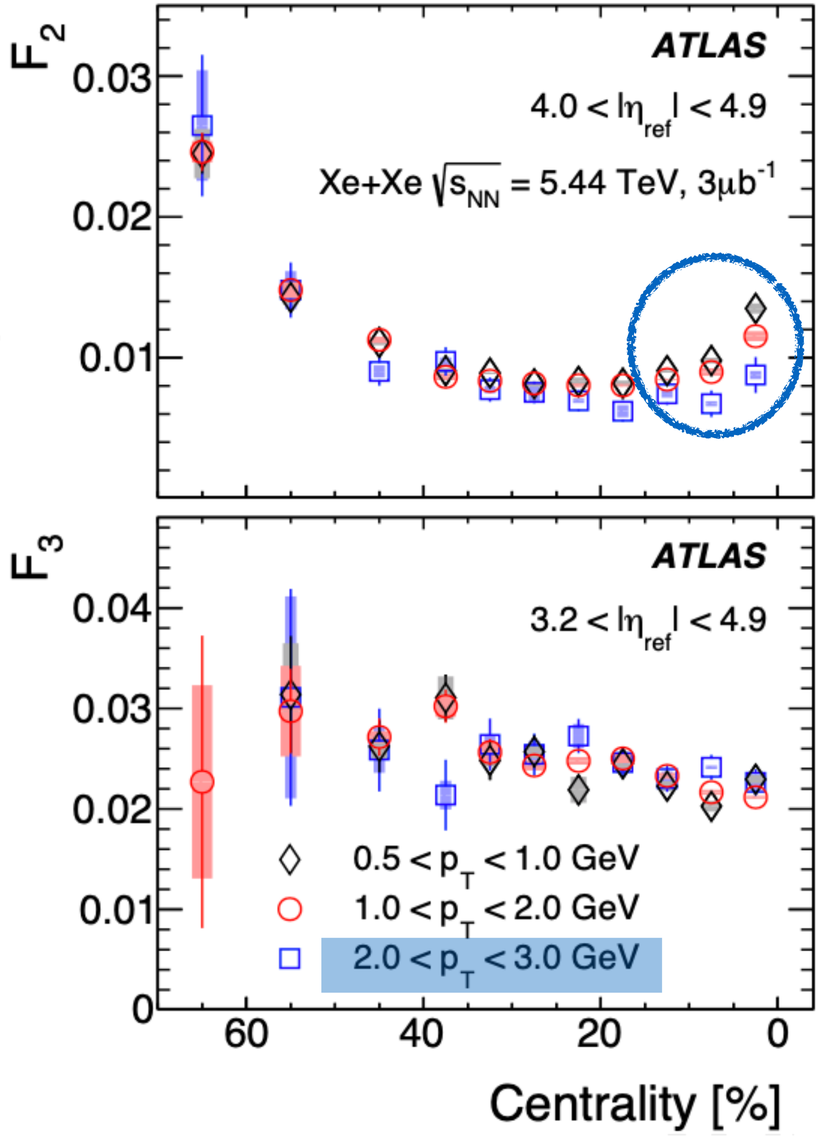

Slope F_n - $|\eta_{ref}|$ and p_T dependence

- Non-flow (dijets) at small $|\eta_{ref}|$ or large p_T

$$r_{n|n}(\eta) = \frac{\langle \mathbf{q}_n(-\eta)\mathbf{q}_n^*(\eta_{ref})\rangle}{\langle \mathbf{q}_n(\eta)\mathbf{q}_n^*(\eta_{ref})\rangle} \uparrow \text{NF} \Rightarrow F_n \uparrow$$

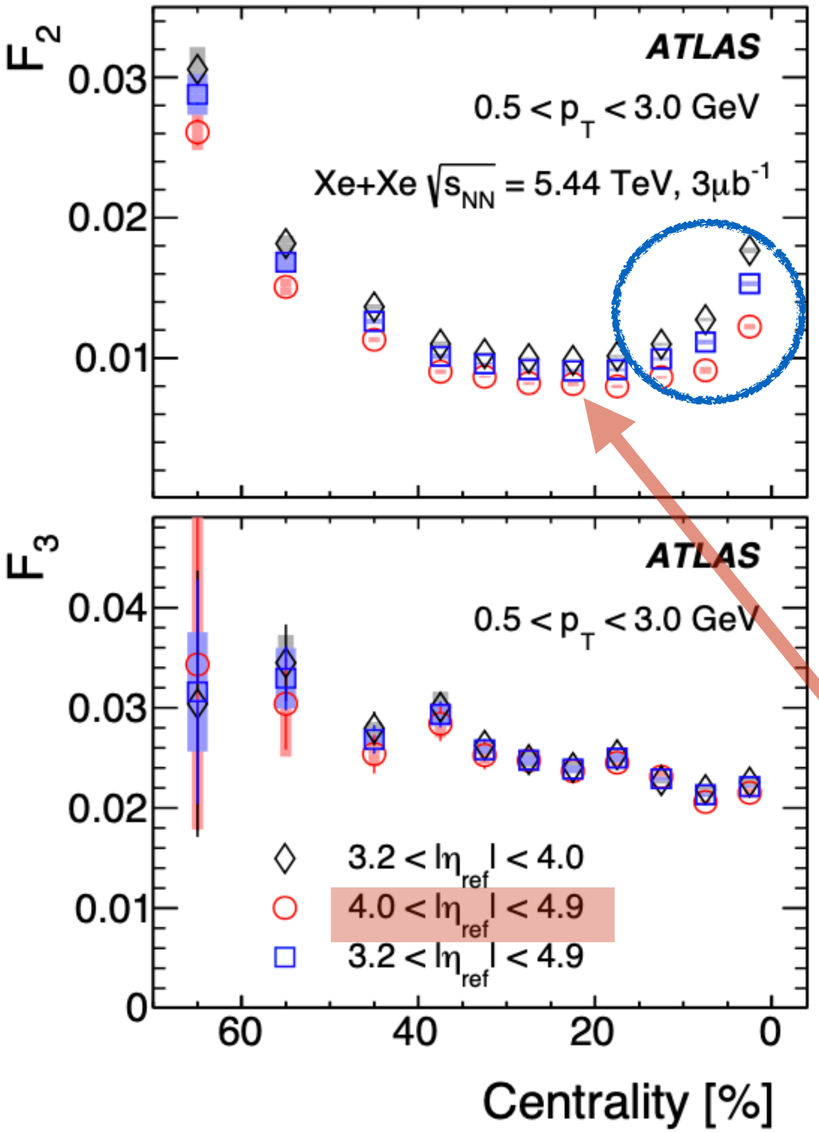

- Larger F_2 at smaller $|\eta_{ref}|$ - NF
- Smaller F_2 at larger p_T - not NF
- Effect larger in central collisions - could be due to non-linear v_2 decorrelation
- F_3 - not affected by NF
- Suppress these variations

$$0.5 < p_{\mathrm{T}} < 3.0\,\mathrm{GeV}$$

$$F_2 \longrightarrow 4.0 < |\eta_{\mathrm{ref}}| < 4.9$$

$$F_3 \longrightarrow 3.2 < |\eta_{\mathrm{ref}}| < 4.9$$

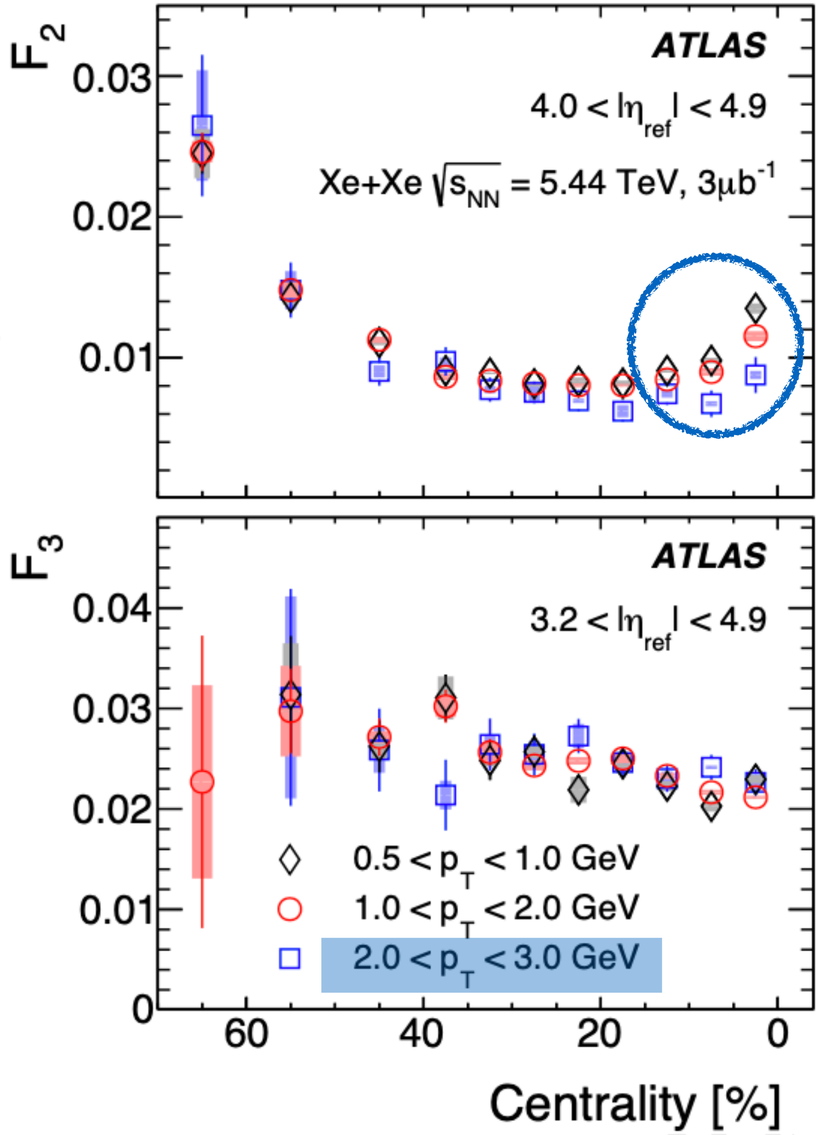

Comparison with Pb+Pb and Hydro

Centrality (avg. geometry)

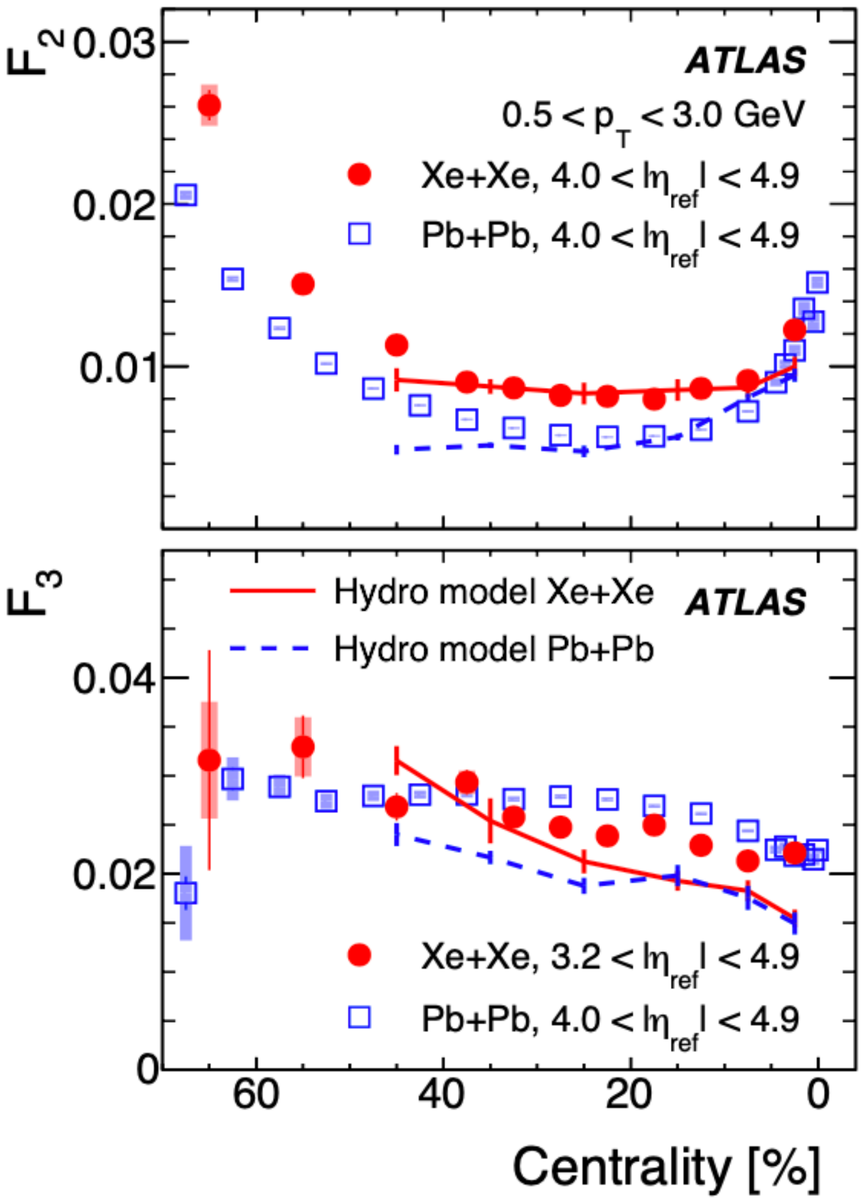

- Reverse ordering for n=2 and 3

$$F_2^{XeXe} > F_2^{PbPb}$$

$$F_3^{XeXe} < F_3^{PbPb}$$

- F_2 and F_3 match - in 0-5% centrality or N_{part} <80

arXiv:1805.03762

N_{part} (system-size)

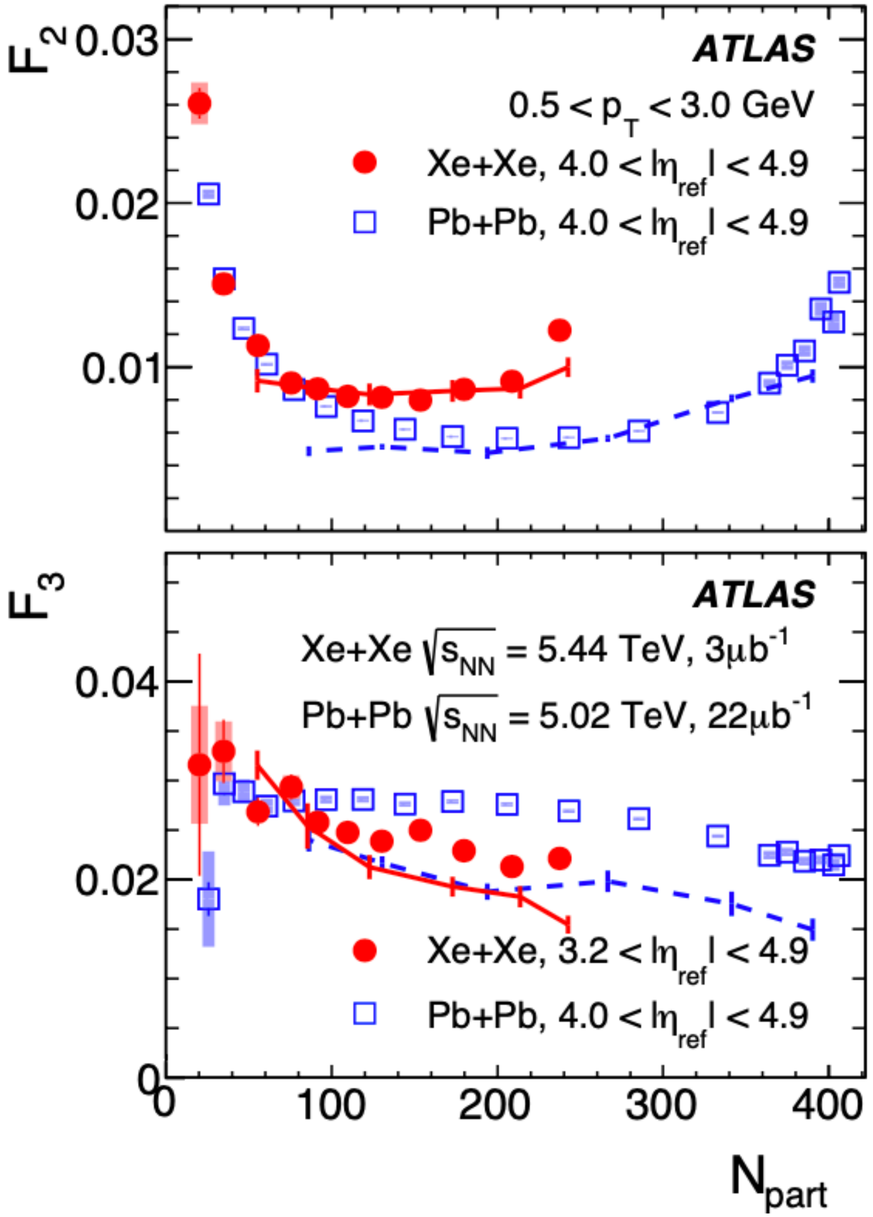

Comparison with Pb+Pb and Hydro

Centrality (avg. geometry)

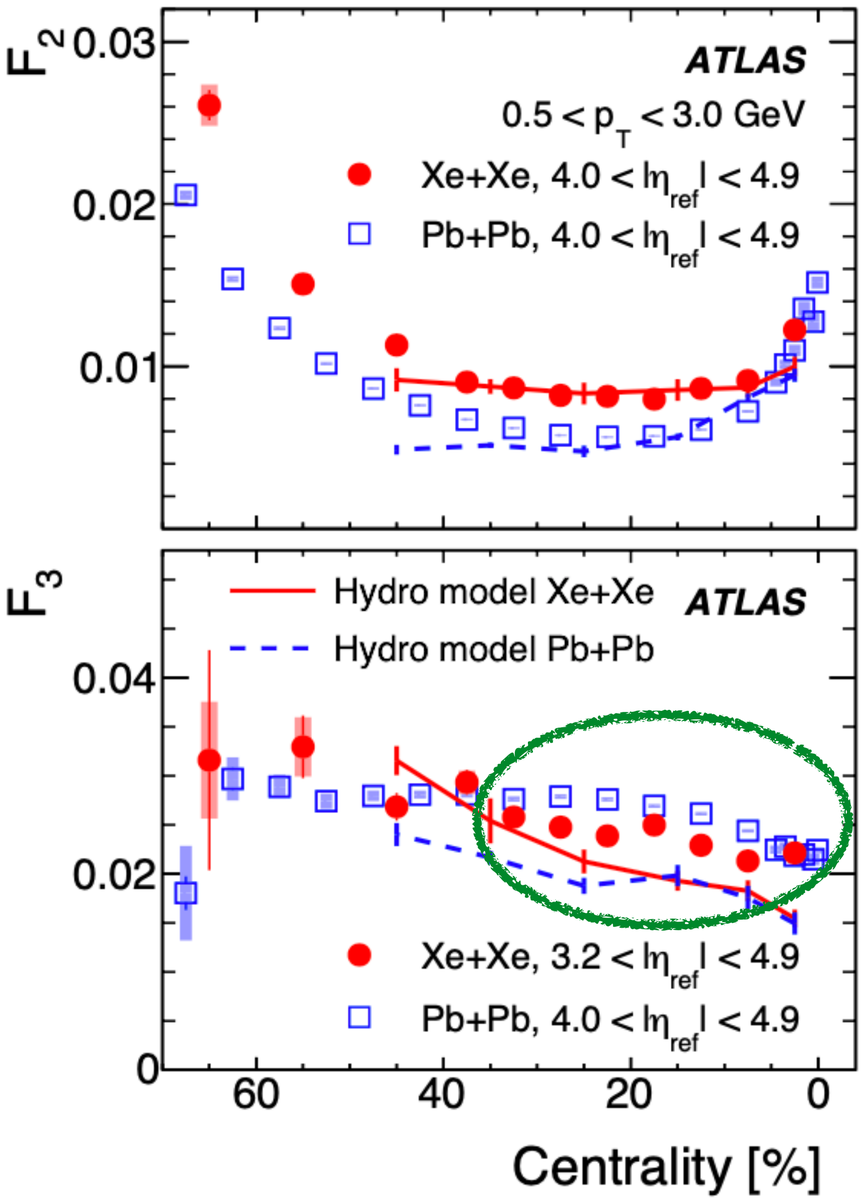

- Reverse ordering for n=2 and 3

$$F_2^{XeXe} > F_2^{PbPb}$$

$$F_3^{XeXe} < F_3^{PbPb}$$

- F_2 and F_3 match - in 0-5% centrality or N_{part} <80

- Hydro model works for F_2 but fails for F_3 in magnitude and splitting

arXiv:1805.03762

N_{part} (system-size)

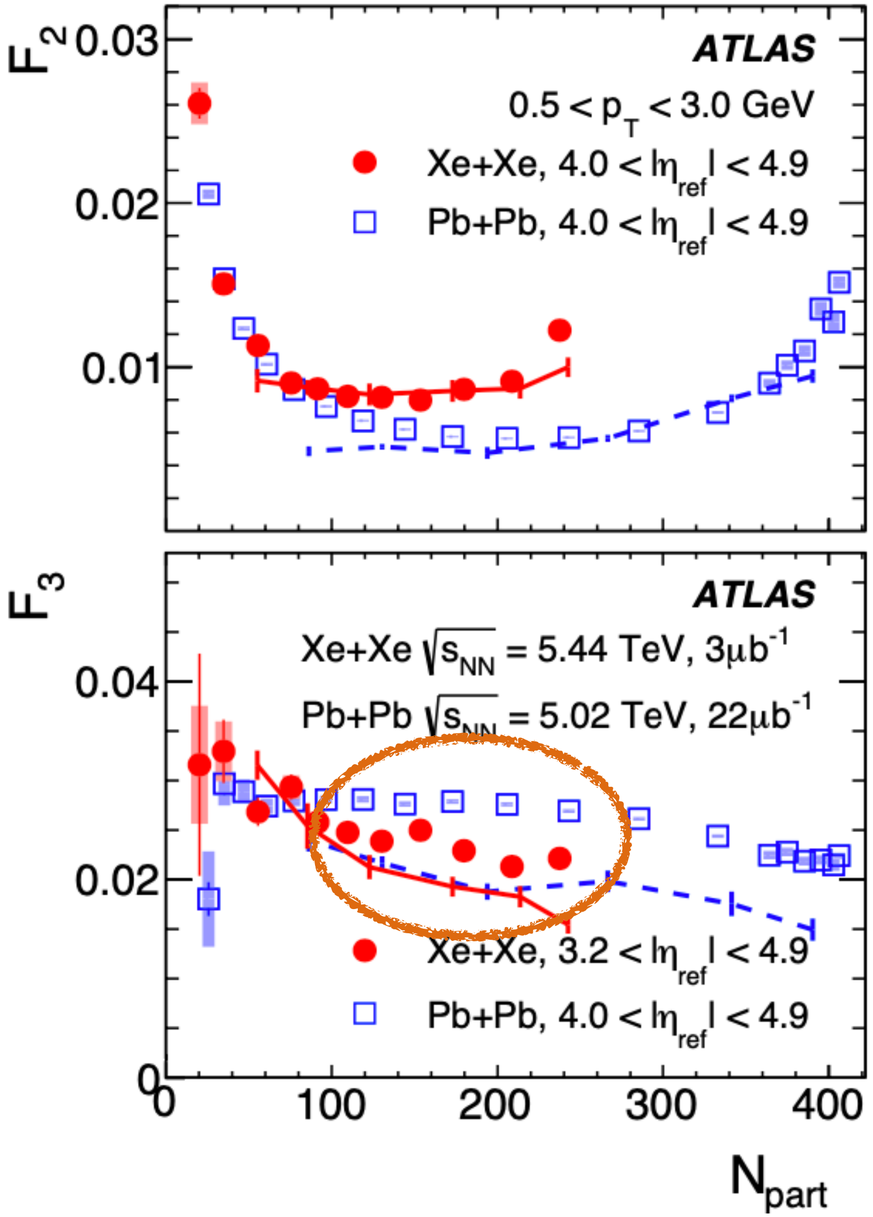

Comparison of v_n and F_n ratios

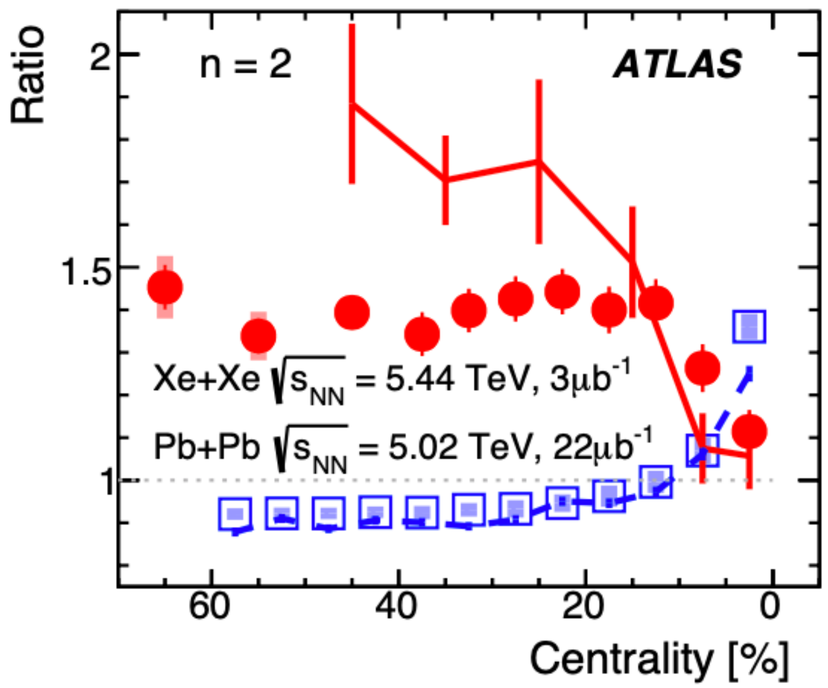

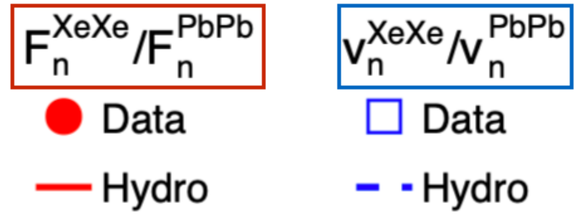

- Anti-correlation between v_n and F_n - opposite centrality dependence

Comparison of v_n and F_n ratios

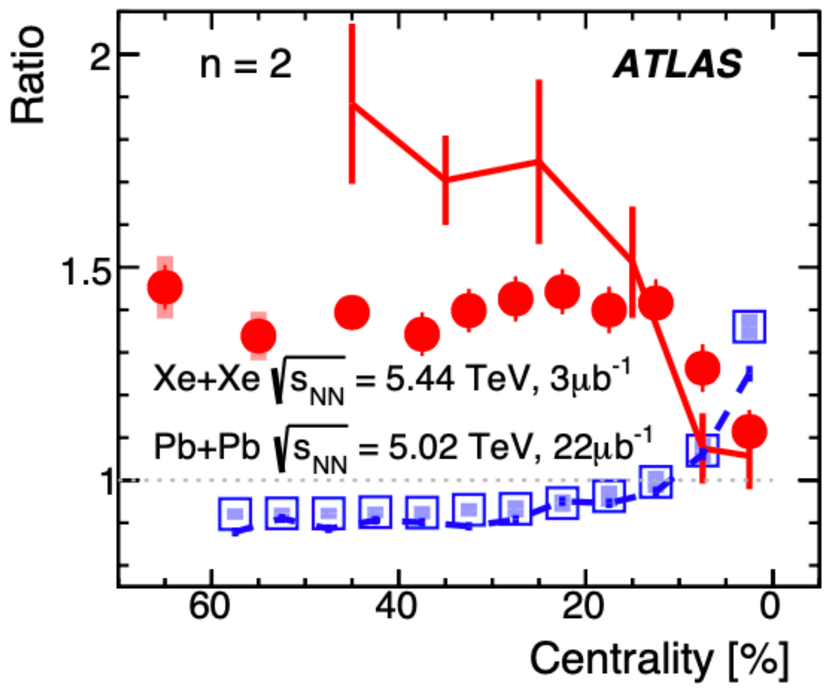

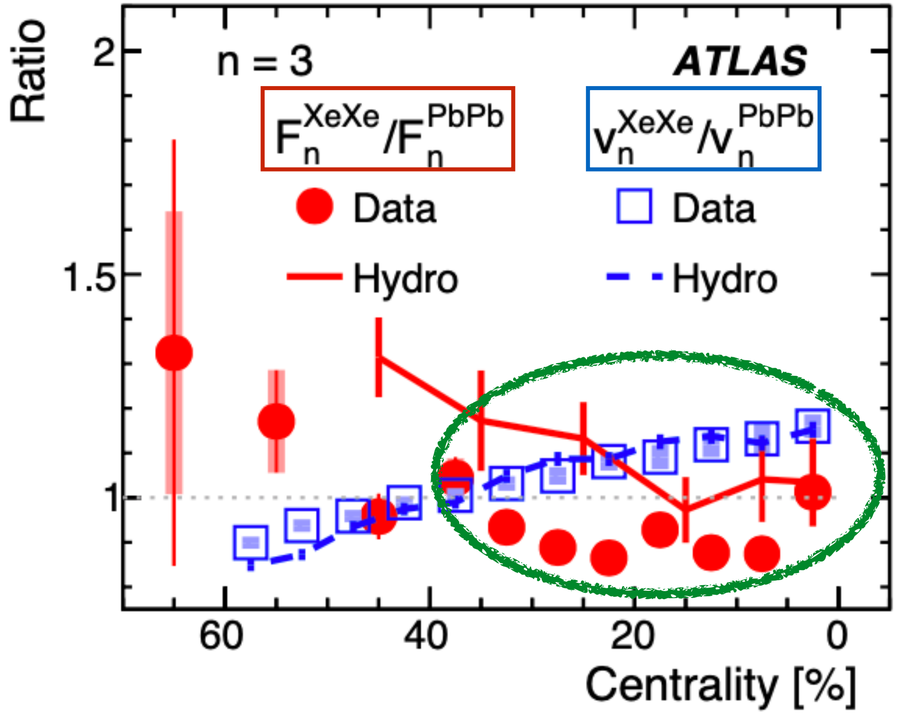

- Anti-correlation between v_n and F_n - opposite centrality dependence
- Reverse ordering of F_2 and F_3 ratios

$$F_2^{XeXe}/F_2^{PbPb} > 1 \qquad F_3^{XeXe}/F_3^{PbPb} < 1$$

- Hydro explains v_n ratio very well but fails to explain F_n ratio accurately
- Whats the origin of the reverse ordering ?

Comparison with Glauber (Initial State)

- Eccentricity ε_n and eccentricity decorrelation A_n from subnucleon-Glauber model arXiv:2003.04340

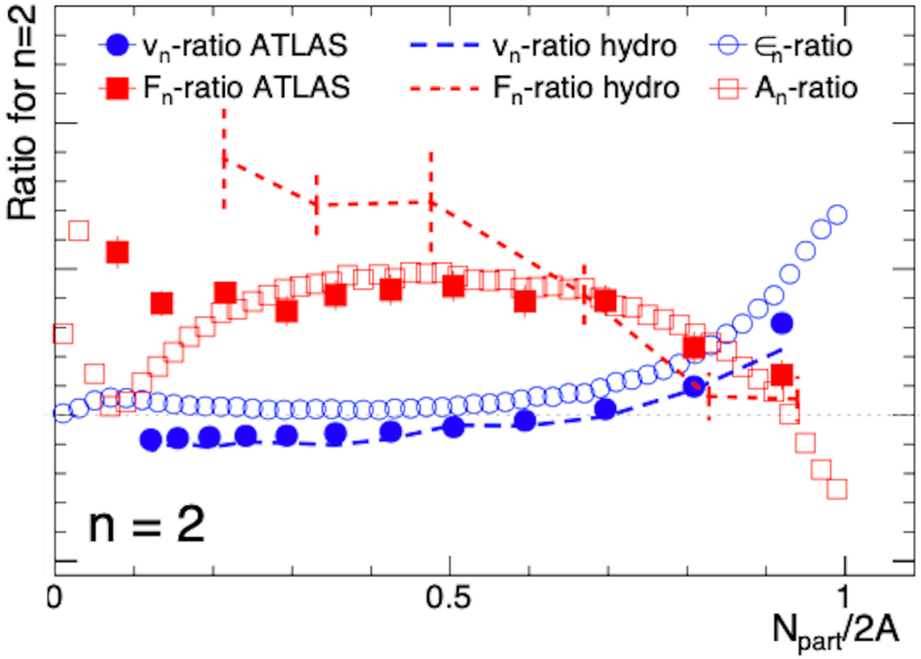

$$\mathcal{E}_{n+} = \frac{\mathcal{E}_n^{\mathrm{F}} + \mathcal{E}_n^{\mathrm{B}}}{2} \quad \mathcal{E}_{n-} = \frac{\mathcal{E}_n^{\mathrm{F}} - \mathcal{E}_n^{\mathrm{B}}}{2}$$

$$A_n \equiv \frac{\langle \varepsilon_{n-}^2 \rangle}{\langle \varepsilon_{n+}^2 \rangle + \langle \varepsilon_{n-}^2 \rangle} \approx \frac{\langle \varepsilon_{n-}^2 \rangle}{\langle \varepsilon_n^2 \rangle}$$

$$\epsilon_n \longrightarrow v_n$$

$$A_n \longrightarrow F_n$$

$N_{part}/2A$ —> Centrality

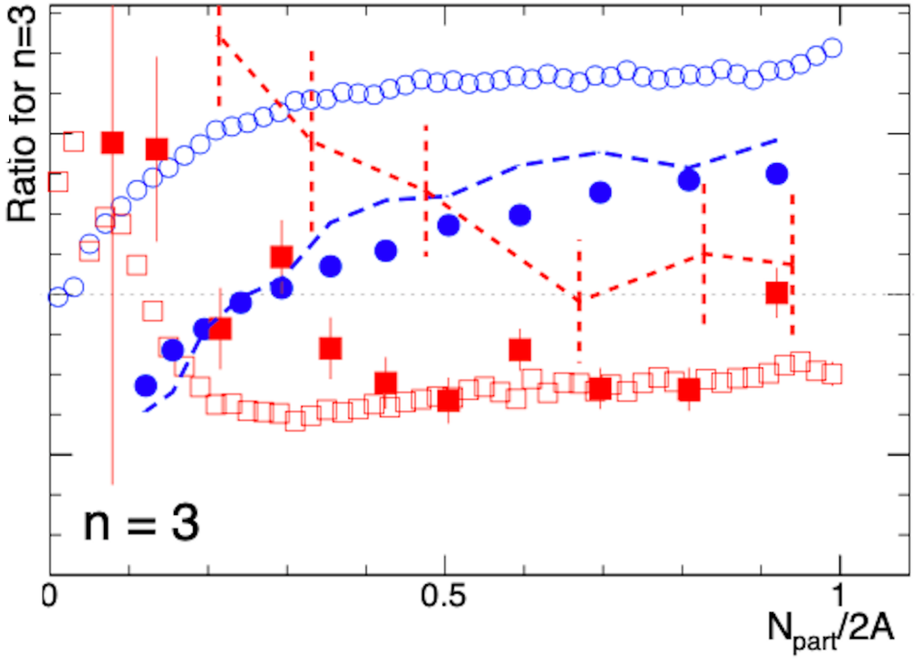

- Difference between v_n and ε_n ratios - Late time effects

Comparison with Glauber (Initial State)

- Eccentricity ε_n and eccentricity decorrelation A_n from subnucleon-Glauber model

arXiv:2003.04340

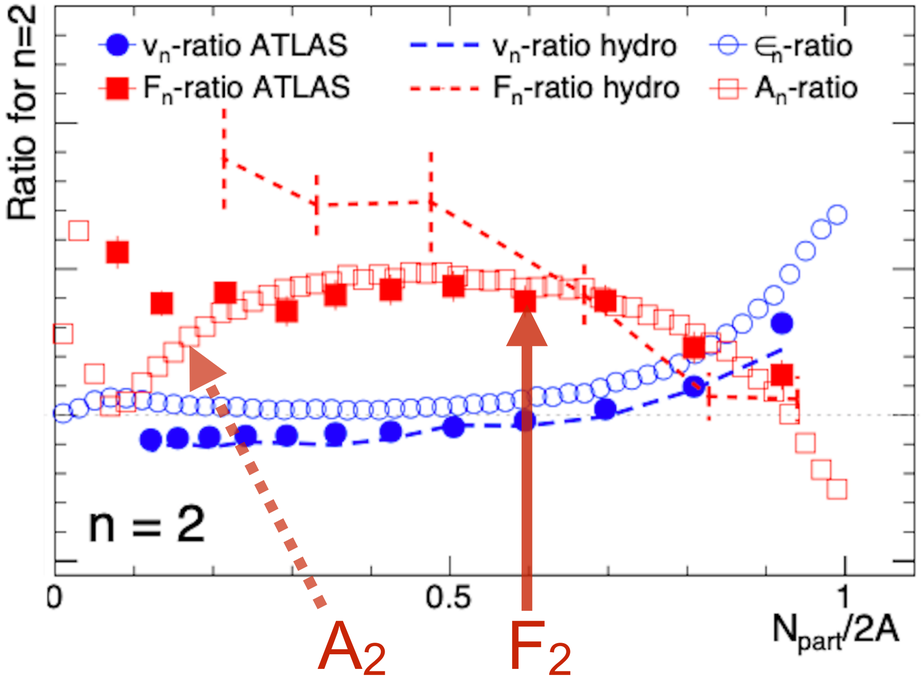

$$\mathcal{E}_{n+} = \frac{\mathcal{E}_n^{\mathrm{F}} + \mathcal{E}_n^{\mathrm{B}}}{2} \quad \mathcal{E}_{n-} = \frac{\mathcal{E}_n^{\mathrm{F}} - \mathcal{E}_n^{\mathrm{B}}}{2}$$

$$A_n \equiv \frac{\langle \varepsilon_{n-}^2 \rangle}{\langle \varepsilon_{n+}^2 \rangle + \langle \varepsilon_{n-}^2 \rangle} \approx \frac{\langle \varepsilon_{n-}^2 \rangle}{\langle \varepsilon_n^2 \rangle}$$

$$\epsilon_n \longrightarrow v_n$$

$$A_n \longrightarrow F_n$$

$N_{part}/2A$ —> Centrality

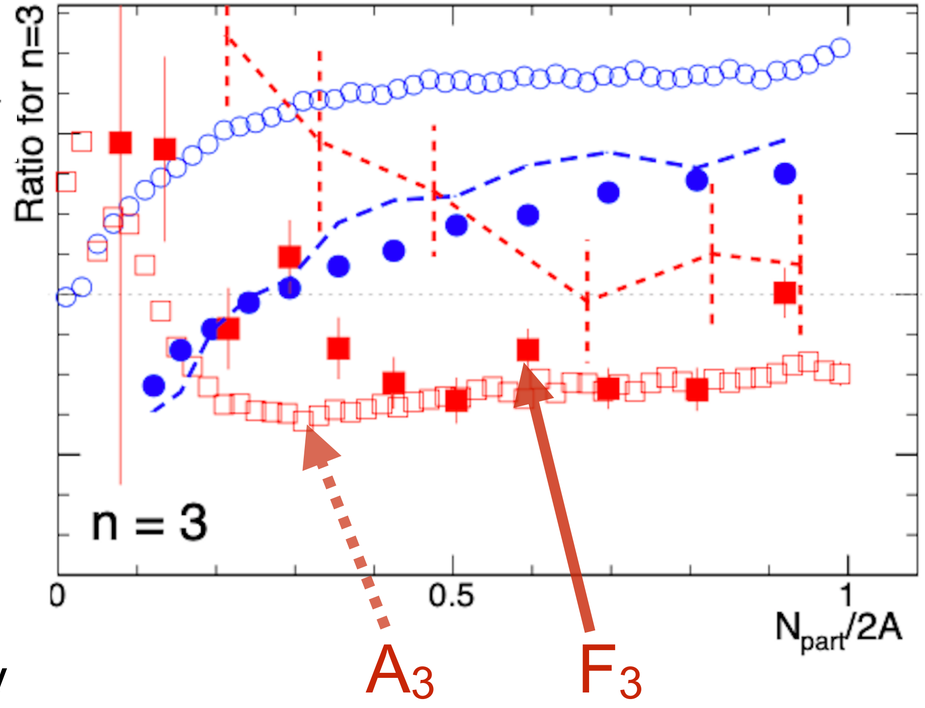

- Difference between v_n and ε_n ratios - Late time effects
- F_n and A_n ratios show good agreement - insensitive to late time effects
- Reverse ordering of ATLAS F_2-F_3 ratios are explained by the Glauber A_2-A_3 ratios
- System-size dependence of F_n - depends mainly on initial state

Summary

- Strong system-size dependence (Xe+Xe vs Pb+Pb) in ATLAS - both v_n and F_n
- Direct comparison v_n and F_n ratios - anti-correlation
- v_n ratios - IS Geometry dominant (central) , Viscous effects dominant (non-central)
- n=2 vs n=3 - same ordering for v_n ratios but reverse ordering for F_n ratios

$$F_2^{XeXe} > F_2^{PbPb}$$

$$F_3^{XeXe} < F_3^{PbPb}$$

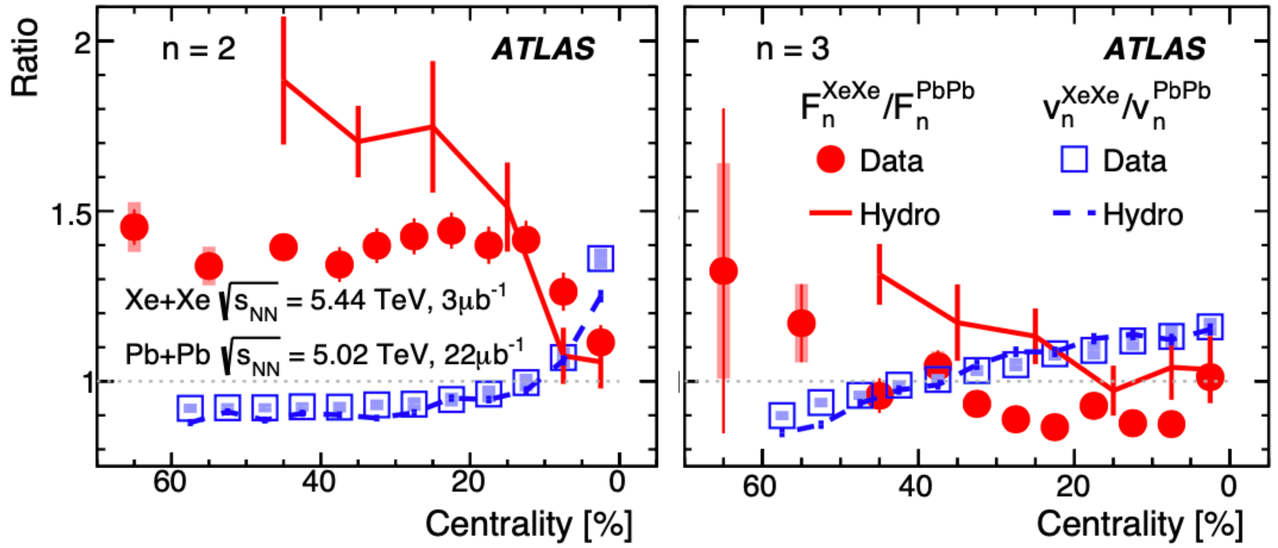

- Current Hydro models tuned for v_n ratio cannot explain F_n ratio accurately
- Glauber Calculation - F_n ratio insensitive to late-time effects, Reverse ordering of n=2,n=3 due to eccentricity decorrelation
- Measurements can constrain different flow models and help develop full 3+1D initial conditions

Backup

Glauber model comparison

- Glauber model calculations compared with ATLAS data and hydro calculations

arXiv:2003.04340

$$\mathcal{E}_n(\eta) = \mathcal{E}_{n+} + f_n(\eta)\mathcal{E}_{n-},\quad \mathcal{E}_{n+} = \frac{\mathcal{E}_n^{\mathrm{F}} + \mathcal{E}_n^{\mathrm{B}}}{2}\quad \mathcal{E}_{n-} = \frac{\mathcal{E}_n^{\mathrm{F}} - \mathcal{E}_n^{\mathrm{B}}}{2}$$

$$r_n^{\mathrm{s}}(\eta) \approx 1 - 2\eta a_n A_n\ , a_n = \left\langle \frac{\partial f_n}{\partial \eta}|_{\eta=0} f_n(\eta_{\mathrm{r}}) \right\rangle\ ,$$

$$A_n \equiv \frac{\langle \varepsilon_{n-}^2 \rangle}{\langle \varepsilon_{n+}^2 \rangle + \langle \varepsilon_{n-}^2 \rangle} \approx \frac{\langle \varepsilon_{n-}^2 \rangle}{\langle \varepsilon_n^2 \rangle}$$

$$\sqrt{\langle v_n^2 \rangle} = \kappa_n \sqrt{\langle \varepsilon_n^2 \rangle} \qquad F_n = \kappa_n' A_n$$

$$\frac{v_n^{\mathrm{A+A}}}{v_n^{\mathrm{B+B}}} = \frac{\kappa_n^{\mathrm{A+A}}}{\kappa_n^{\mathrm{B+B}}} \frac{\varepsilon_n^{\mathrm{A+A}}}{\varepsilon_n^{\mathrm{B+B}}}\ , \frac{F_n^{\mathrm{A+A}}}{F_n^{\mathrm{B+B}}} = \frac{\kappa_n'^{\mathrm{A+A}}}{\kappa_n'^{\mathrm{B+B}}} \frac{A_n^{\mathrm{A+A}}}{A_n^{\mathrm{B+B}}}$$

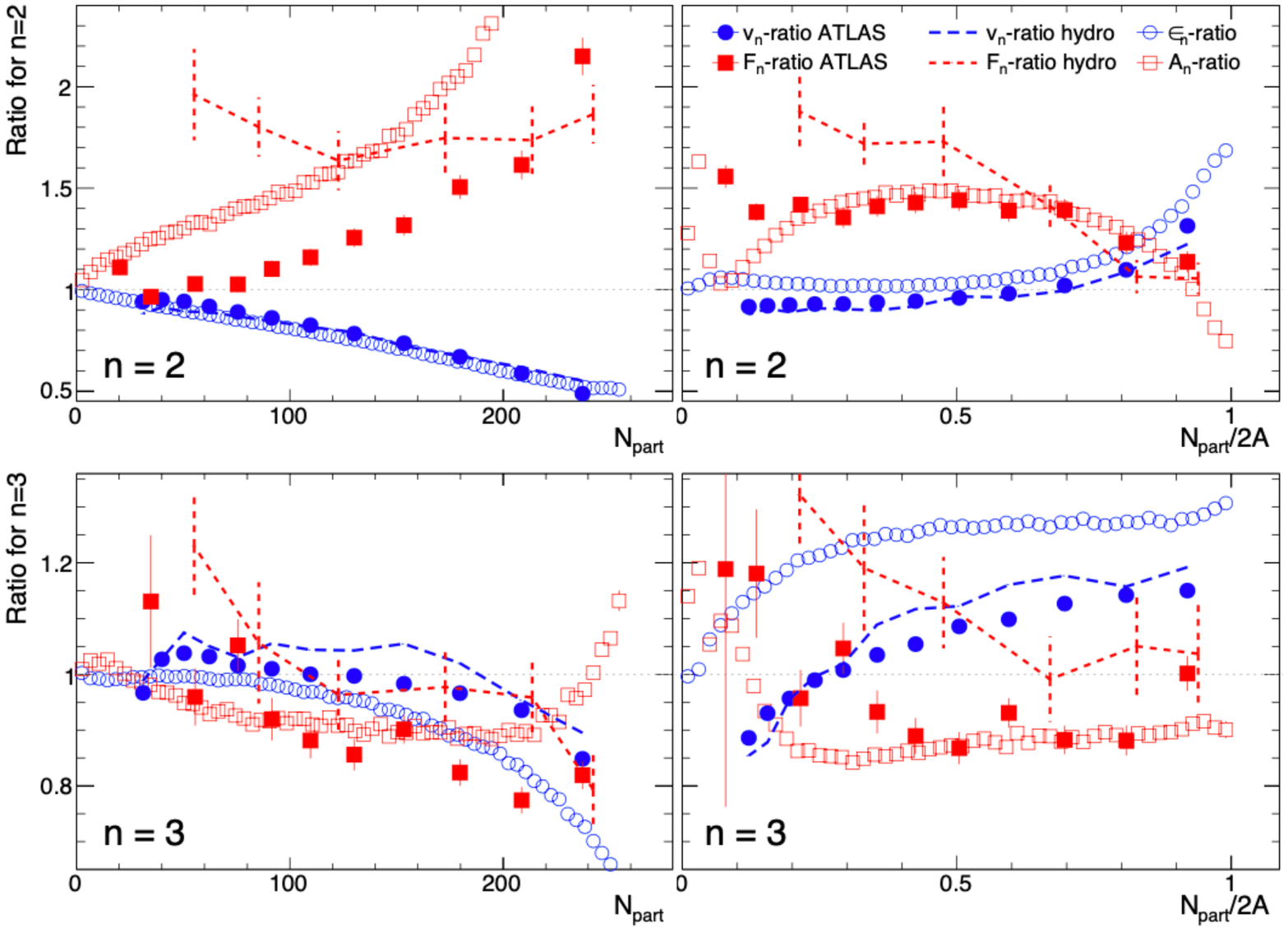

- Opposite ordering of F_2 and F_3 ratios are well reproduced by en and An

Method - 2PC

- 2-particle Correlation

$$C(\Delta\eta, \Delta\phi) = \frac{S(\Delta\eta, \Delta\phi)}{B(\Delta\eta, \Delta\phi)}$$

Integrate with $|\Delta\eta| > 2$ - remove short-range non-flow

$$C(\Delta\phi) = C_0\left[1 + 2\Sigma_{n=1}^{\infty} v_{n,n}\left(p_{\mathrm{T}}^{\mathrm{a}}, p_{\mathrm{T}}^{\mathrm{b}}\right)\cos(n\Delta\phi)\right]$$

✦ Long-range Non-flow (dijets) - peripheral collisions and/or at p_T > 4GeV

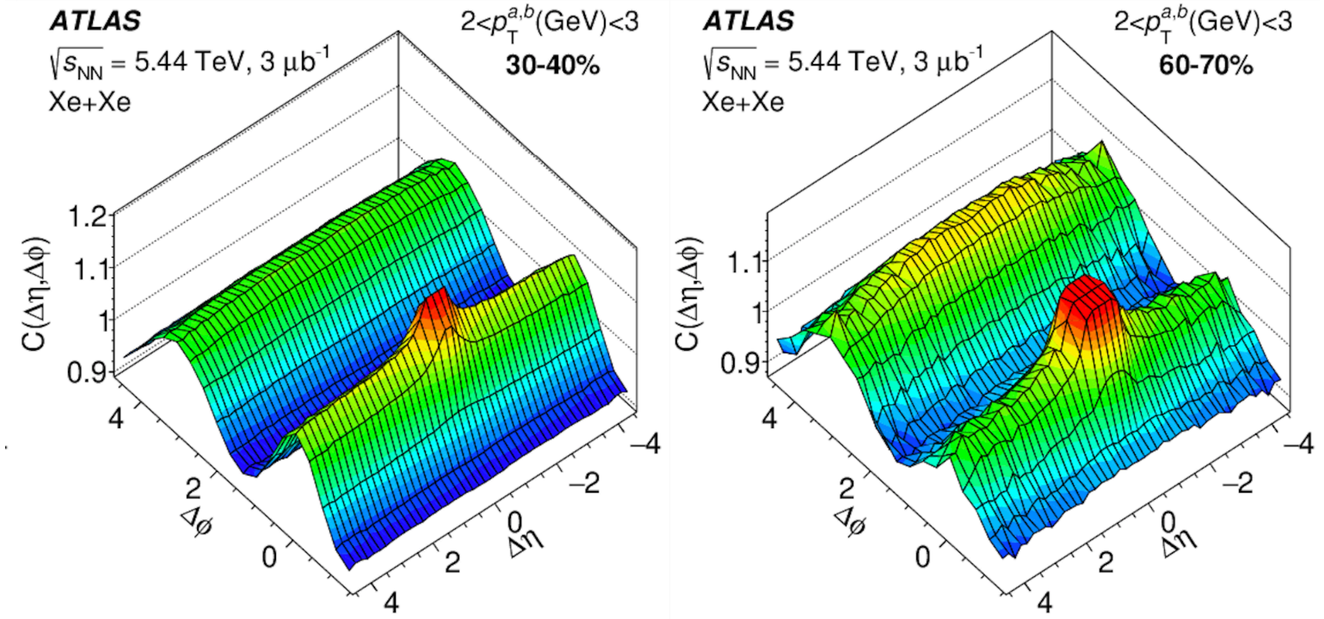

- Template fit method is also implemented

✦ Developed for pp collisions

✦ Can be applied to estimate dijet correlation bias in v_n measurements

✦ Significant for Xe+Xe collisions

$$C^{\mathrm{templ}}(\Delta\phi) \equiv FC^{\mathrm{periph}}(\Delta\phi) + C^{\mathrm{ridge}}(\Delta\phi)$$
$$= FC^{\mathrm{periph}}(\Delta\phi) + G\left[1 + 2\Sigma_{n=2}^{\infty} v_{n,n}\cos(n\Delta\phi)\right]$$

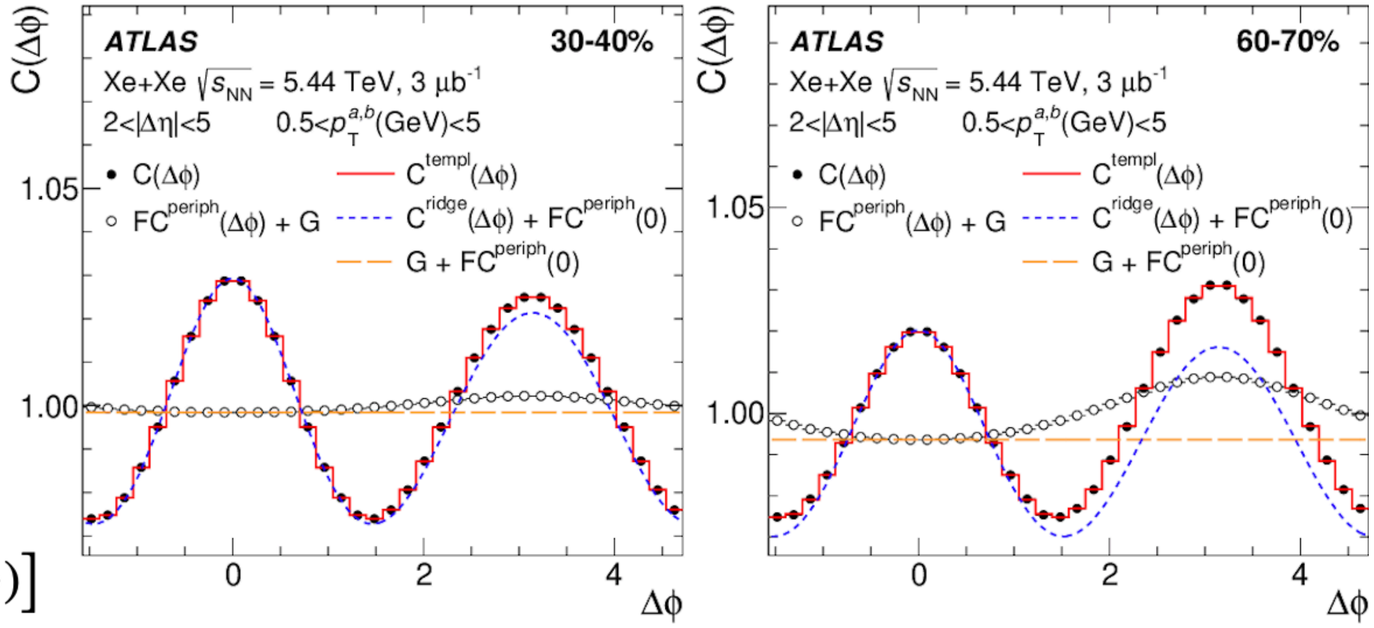

Differential v_n (p_T)

- Assume factorization

$$v_n\left(p_{\mathrm{T}}^{\mathrm{b}}\right) = \frac{v_{n,n}\left(p_{\mathrm{T}}^{\mathrm{a}}, p_{\mathrm{T}}^{\mathrm{b}}\right)}{v_n\left(p_{\mathrm{T}}^{\mathrm{a}}\right)} = \frac{v_{n,n}\left(p_{\mathrm{T}}^{\mathrm{a}}, p_{\mathrm{T}}^{\mathrm{b}}\right)}{\sqrt{v_{n,n}\left(p_{\mathrm{T}}^{\mathrm{a}}, p_{\mathrm{T}}^{\mathrm{a}}\right)}}$$

- Plots - p_T dependence of v_n obtained from 2PC and from template fitting (with and without ZYAM)

- 2PC - Large jet-bias at high-p_T in peripheral collisions, most prominant for v_2 and v_4

- Template fitting - reduces this jet bias